The Meteoritical Society

Meteoritics & Planetary Science 46, Nr 5, 729–736 (2011)
doi: 10.1111/j.1945-5100.2011.01186.x

Planar deformation features in quartz from impact-produced polymict breccia of the Xiuyan crater, China

Ming CHEN[1*], Christian KOEBERL[2,3], Wansheng XIAO[1], Xiande XIE[1], and Dayong TAN[1]

[1]Guangzhou Institute of Geochemistry, Chinese Academy of Sciences, Guangzhou 510640, China
[2]Department of Lithospheric Research, University of Vienna, Althanstrasse 14, A-1090 Vienna, Austria
[3]Natural History Museum, Burging 7, A-1010 Vienna, Austria
[*]Corresponding author. E-mail: mchen@gig.ac.cn

(Received 15 September 2010; revision accepted 01 January 2011)

Abstract–The 1.8 km-diameter Xiuyan crater is an impact structure in northeastern China, exposed in a Proterozoic metamorphic rock complex. The major rocks of the crater are composed of granulite, hornblendite, gneiss, tremolite marble, and marble. The bottom at the center of the crater covers about 100 m thick lacustrine sediments underlain by 188 m thick crater-fill breccia. A layer of polymict breccia composed of clasts of granulite, gneiss, hornblendite, and fragments of glass as well as clastic matrix, occurs near the base, in the depth interval from 260 to 295 m. An investigation in quartz from the polymict breccia in the crater-fill units reveals abundant planar deformation features (PDFs). Quartz with multiple sets of PDFs is found in clasts of granulite that consist of mainly quartz and feldspar, and in fine-grained matrix of the impact-produced polymict breccia. A universal stage was used to measure the orientation of PDFs in 70 grains of quartz from five thin sections made from the clasts of granulite of polymict breccia recovered at the depth of 290 m. Forty-four percent of the quartz grains contain three sets of PDFs, and another 40% contain two sets of PDFs. The most abundant PDFs are rhombohedron forms of $\pi\{10\bar{1}2\}$, $\omega\{10\bar{1}3\}$, and $r/z\{10\bar{1}1\}$ with frequency of 33.5, 22.3, and 9.6%, respectively. A predominant PDF form of $\{10\bar{1}2\}$ in quartz suggests a shock pressure >20 GPa. The occurrence of PDFs in quartz from the polymict breccia provides crucial evidence for shock metamorphism of target rocks and confirms the impact origin of this crater, which thus appears to be the first confirmed impact crater in China.

INTRODUCTION

The shock metamorphic effects in rocks and minerals are the only known means of definitely identifying terrestrial impact craters, and they have been used to identify more than 175 terrestrial craters so far. The shock metamorphic features effectively used for identifying terrestrial impact craters include high-pressure mineral polymorphs, planar deformation features (PDFs) in quartz, diaplectic quartz, and feldspar glasses, and shatter cones (French 1998). Several possible impact structures have been previously reported in China (Wu 1988, 1989; He et al. 1990; Wang 1997; Qin et al. 2001). However, none of them has been confirmed by the discovery of definite shock effects.

Quartz is a common rock-forming mineral in many terrestrial rocks, especially for those occurring in Earth's crust and upper mantle. At shock pressure between 10 and 35 GPa, quartz develops PDFs along specific rational crystallographic orientations (Stöffler and Langenhorst 1994; Grieve et al. 1996). In nature, PDFs in quartz can only be produced through shock metamorphism, and not by any other geological process. Because of widespread occurrence of quartz on Earth's surface, the shock effects of quartz have played a key role in confirmation of many terrestrial impact structures (Chao et al. 1960; Chao 1967; French and Short 1968; Engelhardt and Bertsch 1969; Stöffler and Langenhorst 1994; Grieve et al. 1996; Koeberl 2002; Reimold et al. 2003). The presence of PDFs in quartz

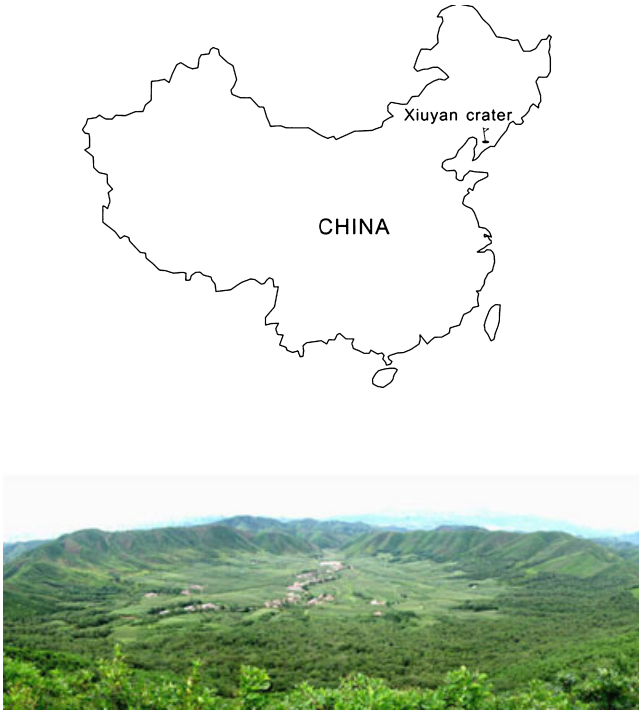

Fig. 1. Location of the Xiuyan crater in China (top) and a panoramic view of the crater as seen from the west (bottom). The diameter of the crater is about 1.8 km.

from the target rocks has been widely accepted to be a diagnostic evidence for evaluating the impact origin of geological structures (Carter 1965; Chao 1967; French and Short 1968; Hörz 1968; Engelhardt and Bertsch 1969; Stöffler 1972; Kieffer et al. 1976; Stöffler and Langenhorst 1994; Grieve et al. 1996; Huffman and Reimold 1996; Koeberl 2002; French and Koeberl 2010).

The Xiuyan crater is located at 40°21′55″N, 123°27′34″E in the Liaodong Peninsula in northeastern China (Fig. 1). It is a simple bowl-shaped crater situated in a low mountain-hill region (Chen et al. 2010a). A narrow gap at the northeastern rim is the main entrance into the inner crater. The rim of the crater is mostly mantled with weathering soil and debris, where it is overgrown with grass and mulberry trees. The crater floor is covered with Quaternary marshy-lacustrine sediments. A small village is situated on the crater floor. The ^{14}C dating of bulk organic matter in the mud/silt clays sampled from the top to the bottom of lacustrine-sediment units (107 m thick) give an age from 39 kyr to around 50 kyr (Chen et al. 2010b). The age of approximately 50 kyr is more likely an infinite age than the true age of the crater as it is close to the limit of radiocarbon dating. The true age of the crater could be >50 kyr. However, this issue remains to be resolved through $^{40}Ar/^{39}Ar$ dating of shock-produced silicate glass.

Chen (2008) conducted the first search for shock metamorphic features in rocks from this crater, and reported the first findings of weathered polymict breccia and one set of PDFs in quartz in deformed basement rocks on the inner wall of crater rim. In 2009, the crater-fill units of nearly 200 m thickness were revealed through a drilling at the center of the crater, from which impact-produced polymict breccia was identified (Chen et al. 2010a). Abundant coesite coexisting with the shock-produced silica glasses has subsequently been found in the gneiss clasts of the polymict breccia recovered in the deep borehole of the Xiuyan crater (Chen et al. 2010b). In this paper, we report the discovery of definite shock effects (PDFs) in quartz from the polymict breccia recovered in the drill cores of the crater.

GEOLOGY OF THE CRATER

The Xiuyan crater is a circular structure with a rim-to-rim diameter of about 1800 m. The maximum rim elevation above the crater floor is 200 m and about 150 m in average. The rock types in a wider area surrounding the crater are composed of the Proterozoic metamorphic rocks of granulite (i.e., leucoleptite—Chen et al. 2010a), hornblendite, gneiss, tremolite marble, and marble (Fig. 2). A composite laccolith of granite and diorite, which were formed in the Triassic period (i.e., the Yanshanian period in China), is located on the west of the crater. The granulite, gneiss, hornblendite, and tremolite marble are major rocks encountered immediately under and around the crater itself. Very limited exposed bedrock can be found in and around the crater because of very thick lacustrine sediments on the crater floor and very thick weathering soil mantled on the most rim area. A few exposed bedrocks mainly made up of granulite and gneiss at the rim show heavy fracturing and in situ brecciation. A possible shatter cone (several centimeters in size) was reported in granulite located at the inner rim (Chen 2008). A drilling positioning at the center of the crater was available in 2009 which reveals the geological structure and stratum of the crater (Chen et al. 2010a).

Figure 3 shows a schematic stratigraphic column from drill core and borehole data (Chen et al. 2010a). After penetrating 107 m of lacustrine sediments, unconsolidated fragments of crystalline basement up to 30 cm in size together with fine-grained clasts and sands were encountered in the depth interval from 107 m to 260 m. These rock fragments consist mainly of granulite, hornblendite, gneiss, and tremolite marble. A few pieces of polymict breccia are also recovered from this interval. A layer enriched in polymict breccia,

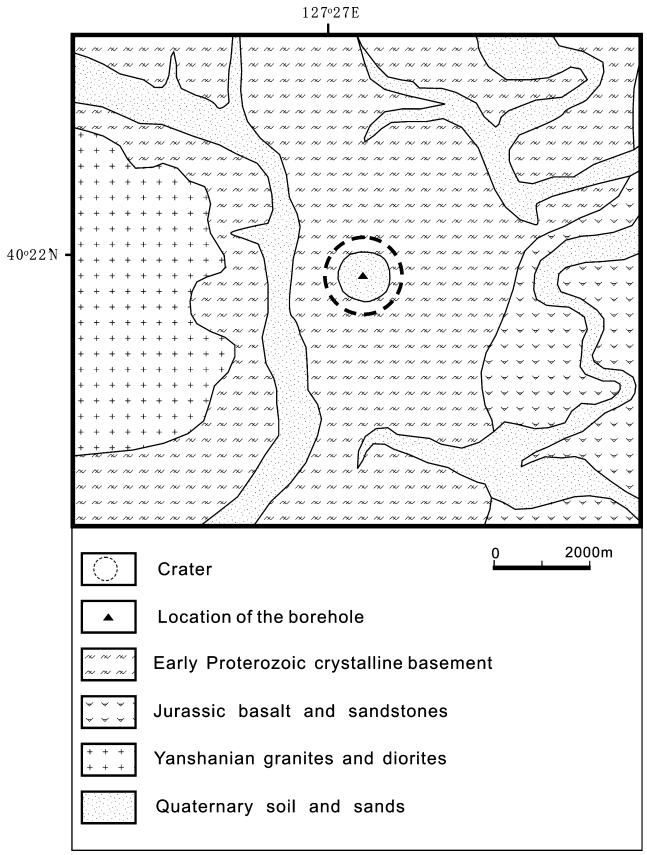

Fig. 2. Schematic geological map around the Xiuyan crater based on the Team No. 1 of Regional Geological Survey (1976).

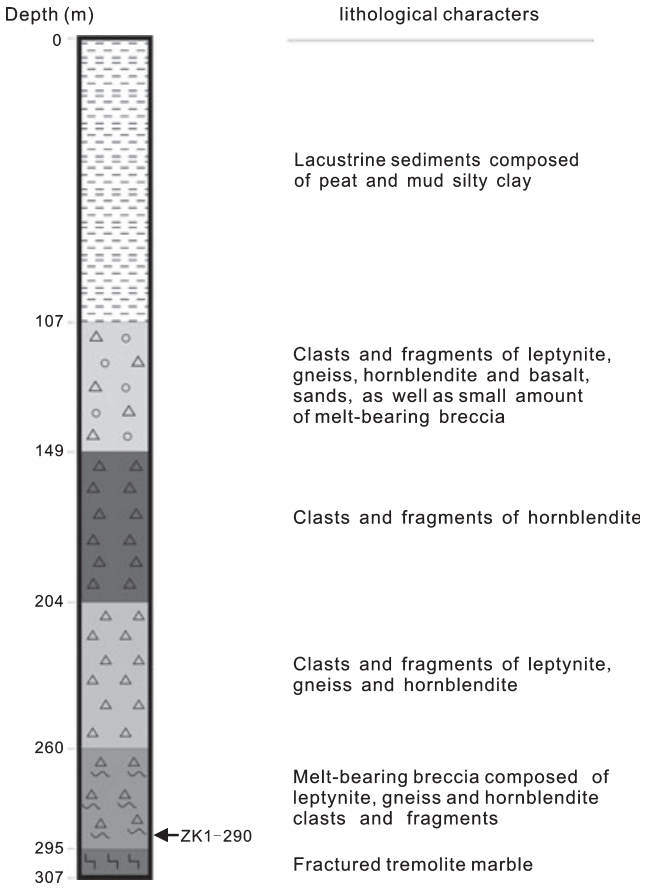

Fig. 3. Schematic stratigraphy of the borehole drilled at the center of the crater. ZK1-LP290 shows the location of the sample analyzed in this study.

which is composed of clasts of granulite, gneiss, hornblendite, and fragments of glass as well as clastic matrix, was encountered in the depth interval from 260 to 295 m. In the interval from 295 to 307 m are fragments or blocks of tremolite marble, which might represent fractured bedrock or coarse blocks of breccia at the crater bottom. The drilling at the center of the crater reveals the crater-fill units or the breccia lens about 188 m in thickness, and is buried below a thick layer of lacustrine sediments.

Polymict breccia is mainly found in the depth interval from 260 to 295 m. The polymict breccia from this depth interval displays strong shock metamorphic feature, such as shock-produced high-pressure polymorph of coesite in some clasts of gneiss (Chen et al. 2010a). It is found that most quartz grains in clasts of granulite from the breccia contain multiple sets of PDFs. Although a few fragments of polymict breccia have been found in the depth interval from 107 to 260 m, only small amounts of quartz in the breccia show weak shock metamorphic feature, such as 1–2 sets of PDFs. It appears that the polymict breccias in the depth interval from 260 to 295 m are more strongly shocked than those in other depth intervals. Considering a low recovery percent of core in the depth interval from 260 to 289 m, we focus this study on the core sample of ZK1-290.

Figure 4 shows a sample (ZK1-290) of polymict breccia recovered from the drill core at 290 m, which is composed of clasts of granulite, hornblendite, gneiss, fragments and patches of glass, and fine-grained matrix. Two kinds of granulite clasts are identified in the breccia. One is pink-gray granulite mainly composed of feldspar (approximately 65%) and quartz (approximately 35%) based on the estimation of dimension of each mineral observed on the thin sections and in hand specimen, and the other is gray granulite composed of feldspar (approximately 60%), quartz (approximately 30%), and small amounts of hornblende and pyroxene (5–10%). Hornblendite contains 80–90% amphibole and 10–20% plagioclase. The gneiss is composed of approximately 35% quartz glass, approximately 55% feldspar glass, and approximately 10% iron-magnesium oxides. The content of glass fragments in the polymict breccia is less than 2% by

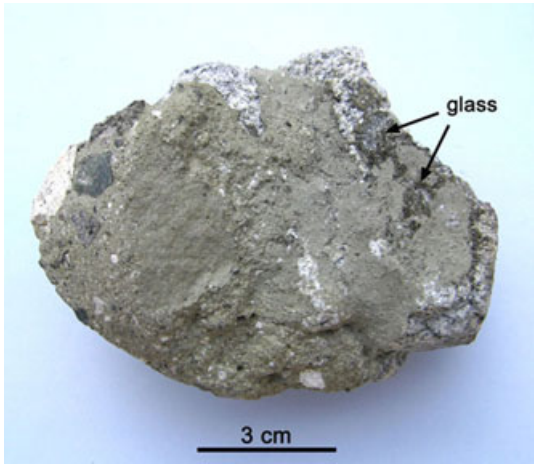

Fig. 4. Polymict breccia composed of clasts of hornblendite, granulite, gneiss, fragments and patches of glass, and fine-grained matrix.

volume. The glass occurs either as fragments of hundred micrometers to millimeters in size in the fine-grained matrix, or as irregular patches up to 2 cm in size. The fine-grained matrix mainly consists of clastic quartz, feldspar, and amphibole, with grain sizes ranging from a few micrometers to millimeters (Fig. 5a). The composition of glass fragments is similar to that of the matrix (Table 1). Since the matrix is a mixture of the relative amounts of different rock types, the composition of glass demonstrates that the glass can in fact be produced from a mixture of the available target rocks.

PDFS IN QUARTZ

A total of 25 polished thin sections of the polymict breccia recovered from the Xiuyan drill core were prepared and investigated under the optical (petrographic) microscope. Quartz with multiple PDFs has been identified in the fine-grained matrix (Fig. 5b) and within the clast of granulite (Fig. 6). The thickness of individual PDF lamellae is 1–2 μm, and the spacing between individual planes ranges from about 1 to 8 μm. The lamella sets are sharp and straight. The PDFs may extend through a whole grain of quartz, or more than half the length of a grain (Figs. 6a and 6b). Many quartz grains are intersected by high density of PDFs with a spacing between individual planes as small as 1 μm (Figs. 6c and 6d). One to five sets of PDFs are observed in a single quartz crystal.

The quartz grains from the clasts of granulite of the polymict breccia contain abundant PDFs. Nearly all grains of quartz show PDFs. Five thin sections of the granulite have been investigated in detail. Among the measured 70 quartz grains, 44% of them contain three sets of PDFs, and 40% contain two sets of PDFs (Fig. 7).

The PDFs in quartz occur in planes corresponding to specific rational crystallographic orientations. The crystallographic orientations of PDFs in quartz grains have been determined with a 4-axis universal stage installed on an optical microscope, according to the methods of Engelhardt and Bertsch (1969), Stöffler and Langenhorst (1994), and Grieve et al. (1996). The optic axis and the poles perpendicular to all sets of PDFs visible in the measured quartz grains were determined, respectively. The *c*-axis and the poles to all sets of PDFs of each quartz grain were plotted on a stereographic Wulff net. The crystallographic orientations of PDFs were indexed using the stereographic projection template displaying the possible pole orientations of common sets of PDFs within a 5° envelope of measurement error using the methods of Ferrière et al. (2009).

A quantity of 70 quartz grains were measured to determine the orientations of poles of 188 planes of PDFs relative to the optical axis. Histogram of angles between *c*-axis and poles to PDFs, binned by 5°, in quartz grains from sample ZK1-LP290 is shown in Fig. 8. Table 2 lists PDFs and the crystallographic indices for these quartz grains, which were obtained from plots of the stereographic Wulff net. A total of 13 forms of PDFs corresponding to rational crystallographic orientations of quartz have been indexed, and these orientations of PDFs include the forms with miller indices of $e\{10\bar{1}4\}$, $\omega\{10\bar{1}3\}$, $\pi\{10\bar{1}2\}$, $\xi\{11\bar{2}2\}$, r, $z\{10\bar{1}1\}$, $s\{11\bar{2}1\}$, $\rho\{21\bar{3}1\}$, $\{22\bar{4}1\}$, $\{31\bar{4}1\}$, $t\{40\bar{4}1\}$, $x\{51\bar{6}1\}$, $m\{10\bar{1}0\}$, and $a\{11\bar{2}0\}$ (Fig. 9). PDFs parallel to the basal (0001) plane are absent. Of all the PDFs measured, 11.2% of them, which did not correspond to rational crystallographic orientations of quartz, were not indexed. The $\{10\bar{1}4\}$ plane, which is indexed by using the revised PDF assignments of Ferrière et al. (2009), is added to the traditional template of Engelhardt and Bertsch (1969). The existence of PDFs parallel to the basal (0001) plane commonly shows a shock pressure less than 10 GPa (Grieve et al. 1996). The absence of the basal (0001) plane in the samples indicates a higher shock pressure.

DISCUSSION

The PDFs in quartz occur in planes corresponding to specific rational crystallographic orientations. Among all indexed sets of PDFs in 70 quartz grains from granulite clasts of polymict breccia, the rhombohedron forms of $\{10\bar{1}2\}$, $\{10\bar{1}3\}$, and $\{10\bar{1}1\}$ have higher frequency percent than other forms. The absolute frequency percent of the form $\{10\bar{1}2\}$ is 33.5%, the one of $\{10\bar{1}3\}$ 22.3%,

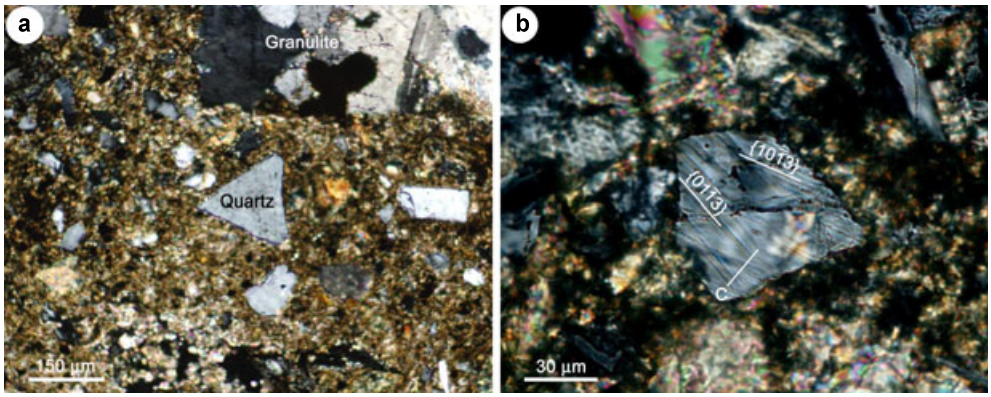

Fig. 5. Fine-grained matrix of polymict breccia, showing clastic quartz clasts, some of which have developed PDFs. a) Angular clasts of granulite and quartz enclosed in fine-grained matrix; cross-polarized light. b) A quartz clast enclosed in fine-grained matrix; cross-polarized light. The quartz is intersected by two sets of PDFs indexed as {10$\bar{1}$3} and {01$\bar{1}$3}, respectively. The white line with "c" is the projection of the quartz *c*-axis in the grain.

Table 1. Chemical composition of Xiuyan polymict breccia, glass fragment, and target rocks.

	Fine-grained matrix	Glass	Granulite-1	Granulite-2	Gneiss	Hornblendite	Tremolite marble
SiO_2	70.11	70.50	77.41	74.12	61.67	49.15	51.20
TiO_2	0.43	0.24	0.24	0.32	0.62	1.32	0.43
Al_2O_3	13.65	13.57	12.29	13.40	14.95	12.98	11.53
Fe_2O_3	3.65	5.95	1.59	2.55	1.90	13.60	11.01
MnO	0.05	0.02	0.01	0.01	0.03	0.15	0.81
MgO	1.64	0.92	0.41	1.00	3.59	7.53	5.34
CaO	1.45	1.51	0.58	0.42	5.94	9.21	11.11
Na_2O	2.57	2.54	5.95	2.68	7.45	2.80	2.34
K_2O	3.29	2.53	0.15	2.78	0.19	1.25	1.14
P_2O_5	0.11	0.03	0.02	0.02	0.15	0.14	1.03
LOI	2.36		0.48	1.93	2.96	1.48	3.91
Total	99.32	97.81	99.14	99.22	99.45	99.58	98.85
Cr	38.3		162.7	< 20	72.2	222.9	74.6
Co	22.8		< 20	< 20	< 20	44.8	89.0
Ni	< 20		< 20	< 20	< 20	40.5	< 20
V	44.3		27.9	< 20	40.6	253.2	136.0
Cu	< 20		< 20	< 20	< 20	< 20	22.3
Zn	22.8		< 20	24.5	25.1	70.3	36.7
Ga	27.5		28.1	28.7	22.5	26.2	21.3
Rb	108.3		< 20	96.3	< 20	54.6	50.4
Sr	67.2		22.6	27.1	88.7	165.4	< 20
Y	27.1		35.6	49.4	14.3	14.9	12.6
Zr	239.8		311.7	337.6	214.7	85.5	62.7
Nb	18		27.7	21.5	16.6	5.6	18.0
Ba	624.1		< 50	213.9	65.9	237.7	624.1

All Fe as Fe_2O_3. Major elements in wt%, trace elements in ppm, determined by X-ray fluorescence. LOI = loss on ignition. Granulite-1 is pink-gray in color in hand specimen, whereas granulite-2 is gray. The composition of glass (average composition in 10 analyses) is determined by electron microprobe analysis.

and the one of {10$\bar{1}$1} 9.6% (Table 2). The predominating forms of PDFs are {10$\bar{1}$2} and {10$\bar{1}$3} (Fig. 9). Among 70 quartz grains, 66% of grains contain rhombohedron {10$\bar{1}$2}, and 43% of grains contain rhombohedron {10$\bar{1}$3}. The predominant occurrence of PDFs {10$\bar{1}$2} + {10$\bar{1}$3} and the absence of PDFs parallel to (0001) indicate a strong shock level or high intensity shock of the samples (Robertson and Grieve 1977; Stöffler and Langenhorst 1994; Grieve et al. 1996). A predominant PDF form of {10$\bar{1}$2} in quartz suggests a

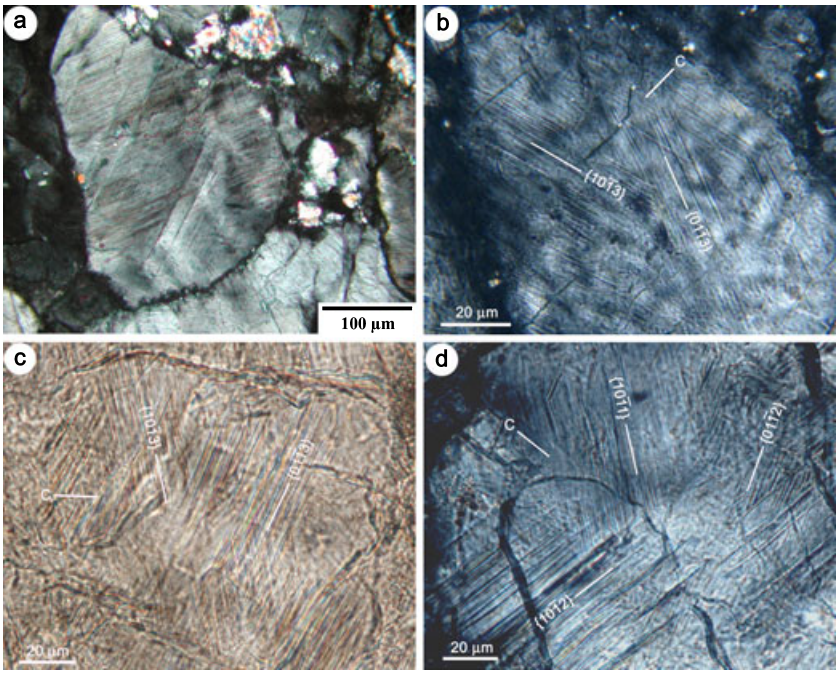

Fig. 6. PDFs in quartz from a clast of granulite. a) Quartz with multiple sets of PDFs, cross-polarized light. b) Two sets of PDFs indexed as $\{10\bar{1}3\}$ and $\{01\bar{1}3\}$, respectively, in a quartz grain; cross-polarized light. c) Two sets of PDFs indexed as $\{10\bar{1}3\}$ and $\{01\bar{1}3\}$, respectively, in a quartz grain, plane-polarized light. d) Three sets of PDFs indexed as $\{10\bar{1}2\}$, $\{01\bar{1}2\}$, and $\{10\bar{1}1\}$, respectively, in a quartz grain, cross-polarized light. The white line with "c" is the projection of the quartz *c*-axis in the grain.

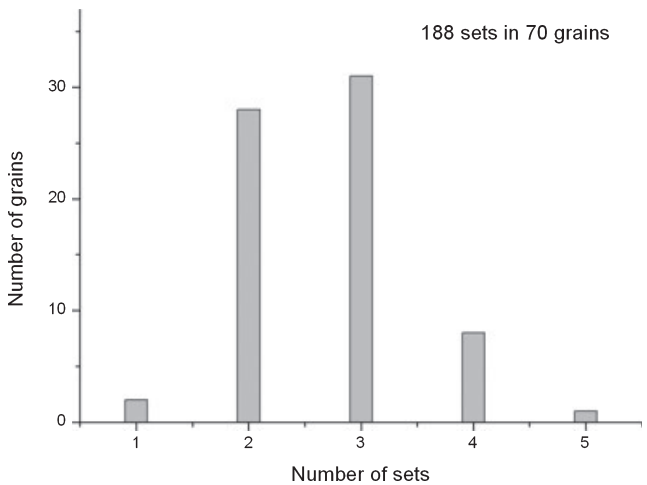

Fig. 7. Histogram of the number of sets of PDFs per individual quartz grain from sample ZK1-LP290.

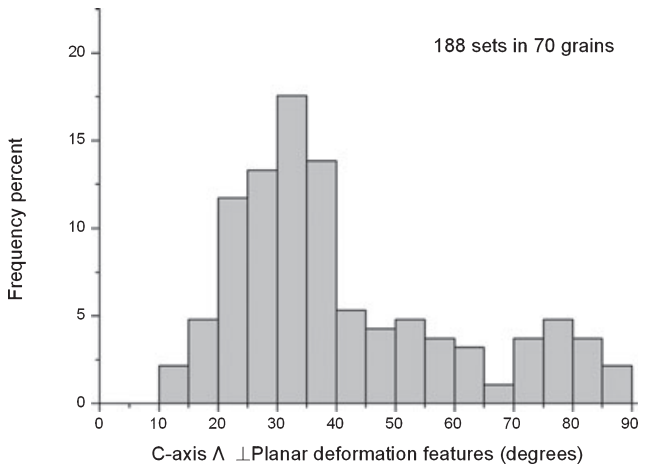

Fig. 8. Histogram of angles between *c*-axis and poles to PDF, binned by 5°, in quartz grains from sample ZK1-LP290.

shock pressure >20 GPa (Grieve et al. 1996). Based on the higher frequency of PDFs $\{10\bar{1}2\}$ in our samples, the shock pressure required for onset of the PDFs could be above 20 GPa. The occurrence of PDFs in the quartz grains is indicative of shock metamorphism in the granulite target rock.

For the target rocks, there is generally a positive correlation between the number of PDF sets in quartz and the magnitude of the shock pressure (Trepmann and Spray 2006; Ferrière et al. 2009). In comparison to one set of PDFs in quartz in the rim of the Xiuyan crater (Chen 2008), predominant multiple sets of PDFs in quartz in the polymict breccia suggest a stronger shock level.

The composition of fine-grained matrix in the polymict breccia shows a combination from target rocks

Table 2. PDFs and crystallographic indices in 70 quartz grains from the clasts of granulite of the polymict breccia of the Xiuyan crater, using the stereographic projection template for the indexing.

Planes and symbols	Miller-Bravais index	Polar angle with *c*-axis	No. of PDFs	Percentage
e	$\{10\bar{1}4\}$	17.62°	6	3.2
ω	$\{10\bar{1}3\}$	22.95°	42	22.3
π	$\{10\bar{1}2\}$	32.42°	63	33.5
ξ	$\{11\bar{2}2\}$	47.73°	5	2.6
r, z	$\{10\bar{1}1\}$	51.79°	18	9.6
s	$\{11\bar{2}1\}$	65.56°	7	3.7
ρ	$\{21\bar{3}1\}$	73.71°	5	2.6
–	$\{22\bar{4}1\}$	77.20°	9	4.8
–	$\{31\bar{4}1\}$	77.91°	2	1.1
t	$\{40\bar{4}1\}$	78.87°	2	1.1
x	$\{51\bar{6}1\}$	82.07°	2	1.1
m, a	$\{10\bar{1}0\}, \{11\bar{2}0\}$	90.00°	6	3.2
Unindexed	–	–	21	11.2
Total	–	–	188	100

including granulite, gneiss, hornblendite, and tremolite marble (Table 1). The compositional similarity between the glass fragments and the fine-grained matrix demonstrates that the glass forms from partial melting of shocked rocks.

Polymict breccias containing glass and crystal or lithic clasts, which form during an impact event, and are composed of shock- and nonshock-metamorphosed minerals and rock fragments from the crystalline basement, have been described as "suevite breccia," a diagnostic rock for impact origin (Stähle 1972; Engelhardt and Graup 1984; Engelhardt et al. 1995). The existence of PDFs in quartz from the polymict breccia from the Xiuyan crater not only establishes unambiguous evidence for shock metamorphism, but also substantiates that the polymict breccia containing glass belongs to a kind of suevite breccia. The PDFs in quartz from the polymict breccia confirm an impact origin of the Xiuyan structure.

The polymict breccia recovered from the drill core at 290 m shows strong shock metamorphic features including high-pressure polymorph of coesite in the clasts of gneiss (Chen et al. 2010b), and multiple sets of PDFs in quartz from clasts of granulite. Both a predominant PDF form of $\{10\bar{1}2\}$ in quartz and coesite could indicate a shock pressure >20 GPa and >30 GPa, respectively (Stöffler and Langenhorst 1994; Grieve et al. 1996). It demonstrates that the polymict breccia experienced high shock pressure. The strong shock metamorphosed effects are usually accompanied by large impact. The Xiuyan crater is a small impact structure with a 1.8 km diameter. The strongly shock metamorphosed rocks from this small

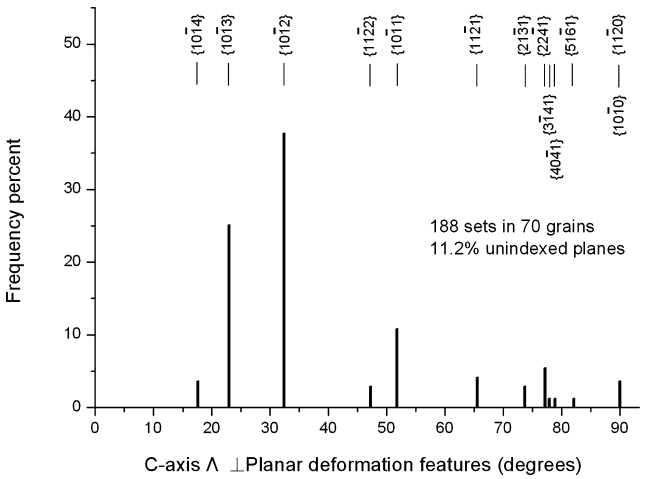

Fig. 9. Histogram of the frequency percent of indexed PDFs in quartz grains from sample ZK1-LP290 using a template of quartz crystallographic indices. The $\{10\bar{1}4\}$ plane is indexed by using the revised PDF assignments of Ferrière et al. (2009).

crater demonstrate that some target rocks, regardless of their relatively small volume, have experienced very high shock pressures, if they are spatially close to the impactor.

Acknowledgments—We thank B. M. French, C. Trepmann, and the AE J. G. Spray for the constructive comments and suggestions, and K. Bartosova (University of Vienna) for assistance with the use of the U-stage. M. C., W. X., X. X., and D. T. are supported by National Natural Science Foundation of China (Grant No. 40872041), Chinese Academy of Sciences (Grant No. Kzcx2-yw-140), and President Foundation of Chinese Academy of Sciences in 2007. The University of Vienna provided partial assistance to M. C. during a research visit in Vienna. This is contribution No. IS-1299 from GIGCAS.

Editorial Handling—Dr. John Spray

REFERENCES

Carter N. L. 1965. Basal quartz deformation lamellae; a criterion for recognition of impactites. *American Journal of Science* 263:786–806.

Chao E. C. T. 1967. Shock effects in certain rock-forming minerals. *Science* 156:192–202.

Chao E. C. T., Shoemaker E. M., and Madsen B. M. 1960. First natural occurrence of coesite. *Science* 132:220–222.

Chen M. 2008. Impact-derived features of the Xiuyan meteorite crater. *Chinese Science Bulletin* 53:392–395.

Chen M., Xiao W., Xie X., Tan D., and Cao Y. 2010a. Xiuyan crater, China: Impact origin confirmed. *Chinese Science Bulletin* 55:1777–1781.

Chen M., Xiao W., and Xie X. 2010b. Coesite and quartz characteristic of crystallization from shock-produced silica

melt in the Xiuyan crater. *Earth and Planetary Science Letters* 297:305–313.

von Engelhardt W. and Bertsch W. 1969. Shock-induced planar deformation structures in quartz from the Ries crater, Germany. *Contributions to Mineralogy and Petrology* 20:203–234.

von Engelhardt W. and Graup G. 1984. Suevite of the Ries crater, Germany: Source rocks and implications for cratering mechanics. *Geologische Rundschau* 73:447–481.

von Engelhardt W., Arndt J., Fecker B., and Pankau H. G. 1995. Suevite breccia from the Ries crater, Germany: Origin, cooling history and devitrification of impact glasses. *Meteoritics* 30:279–293.

Ferrière L., Morrow J. R., Amgaa T., and Koeberl C. 2009. Systematic study of universal-stage measurements of planar deformation features in shocked quartz: Implications for statistical significance and representation of results. *Meteoritics & Planetary Science* 44:925–940.

French B. M. 1998. Traces of Catastrophe: A Handbook of Shock-Metamorphic Effects in Terrestrial Meteorite Impact Structures. LPI Contribution 954. Houston, Texas: Lunar and Planetary Institute. 120 p.

French B. M. and Koeberl C. 2010. The convincing identification of terrestrial meteorite impact structures: What works, what doesn't, and why. *Earth-Science Reviews* 98:123–170.

French B. M. and Short N. M. 1968. *Shock metamorphism of natural materials*. Baltimore: Mono Book Corporation. 644 p.

Grieve R. A. F., Langenhorst F., and Stöffler D. 1996. Shock metamorphism of quartz in nature and experiments: II. Significance in geoscience. *Meteoritics & Planetary Science* 31:6–35.

He Y., Xu D., Lu D., Shen Z., Lin C., and Shi L. 1990. Shock-deformed features of quartz from the Taihu: An investigation for origin of the Taihu In Chinese. *Chinese Science Bulletin* 35:1163–1166.

Hörz F. 1968. Statistical measurements of deformation structures and refractive indices in experimentally shock loaded quartz. In *Shock metamorphism of natural materials*, edited by French B. M. and Short N. M. Baltimore: Mono Book Corporation. pp. 243–253.

Huffman A. R. and Reimold W. U. 1996. Experimental constraints on shock-induced microstructures in naturally deformed quartzites. *Tectonophysics* 256:165–217.

Kieffer S. W., Phakey P. P., and Christie J. M. 1976. Shock processes in porous quartzite: Transmission electron microscope observations and theory. *Contribution to Mineralogy and Petrology* 59:41–93.

Koeberl C. 2002. Mineralogical and geochemical aspects of impact craters. *Mineralogical Magazine* 66:745–768.

Qin G., Lu D., Ou Q., and Chu X. 2001. The discovery of PGE anormaly and platina from Luoquanli impact crater. *Earth Science Frontiers* 8:333–338. In Chinese.

Reimold W. U., Koeberl C., Hough R. M., McDonald I., Bevan A., Amare K., and French B. M. 2003. Woodleigh impact structure, Australia: Shock petrography and geochemical studies. *Meteoritics & Planetary Science* 38:1109–1130.

Robertson P. and Grieve R. A. F. 1977. Shock attenuation at terrestrial impact structures. In *Impact and explosion cratering*, edited by Roddy D. J., Pepin R. O., and Merrill R. B. New York: Pergamon Press. pp. 687–702.

Stähle V. 1972. Impact glasses from suevite, Ries crater, Germany. *Earth and Planetary Science Letters* 17:275–293.

Stöffler D. 1972. Deformation and transformation of rock-forming minerals by natural and experimental shock processes: 1. Behaviour of minerals under shock compression. *Fortschritte der Mineralogie* 49:50–113.

Stöffler D. and Langenhorst F. 1994. Shock metamorphism of quartz in nature and experiment: I. Basic observation and theory. *Meteoritics & Planetary Science* 29:155–181.

Team No. 1 of Regional Geological Survey, 1976. *Xiuyan and Dahushan geological maps (1:200 000), regional geological investigation reports* In Chinese. Shen Yang: Liaoning Geological Bureau. pp. 143–147.

Trepmann C. and Spray J. G. 2006. Shock-induced crystal-plastic deformation and post-shock annealing of quartz: Microstructural evidence from crystalline target rocks of the Charlevoix impact structure, Canada. *European Journal of Mineralogy* 18:161–173.

Wang D. 1997. *Hainan Baisha impact crater* In Chinese. Hainan: Hainan Press. 60 p.

Wu S. 1988. The Shanghewan impact crater, China (abstract). 18th Lunar and Planetary Science Conference. p. 1296.

Wu S. 1989. Geologic feature of the Duolun impact crater, China (abstract). 20th Lunar and Planetary Science Conference. p. 1219.